

Review

Rational Design of Fluorescent/Colorimetric Chemosensors for Detecting Transition Metal Ions by Varying Functional Groups

Jong-Kwon Park ^{1,†}, Junhyeop Shin ^{1,†}, Seohyeon Jang ^{1,†}, Myeong-Lok Seol ², Jihyeon Kang ¹, Seyoung Choi ¹, Hojong Eom ¹, Ohhyun Kwon ¹, Soomin Park ³ , Dong-Youn Noh ^{4,*} and Inho Nam ^{1,*} 

¹ School of Chemical Engineering and Materials Science, Department of Intelligent Energy and Industry, Department of Advanced Materials Engineering, Chung-Ang University, Seoul 06974, Korea

² NASA Ames Research Center, Universities Space Research Association, Moffett Field, CA 94035, USA

³ School of Energy, Materials and Chemical Engineering, Korea University of Technology and Education, Cheonan 31253, Korea

⁴ Department of Chemistry, Seoul Women's University, Seoul 01797, Korea

* Correspondence: dynoh@swu.ac.kr (D.-Y.N.); inhonam@cau.ac.kr (I.N.)

† These authors contributed equally to this work.

Abstract: In recent decades, concerns about increasing biological and environmental contamination have necessitated the development of chemosensors with high selectivity, sensitivity, and cost-effectiveness. In principle, the sensing performance can be affected by the functional group(s) of receptor, the charge of the metal ion(s), and the electron configuration of the sensing molecule(s) and metal ion(s). Fine controlling of the substituents can influence the electron density of the receptor to enhance the binding affinity to metal ions, which is an effective way to improve the photophysical properties of the sensors. This review explores the effect of functional group modification on the performance of various chemosensors represented by Pt(dithiolene)-based complexes (2012–2021). Then, recently developed Schiff base chemosensors (2014–2021) are discussed. The Schiff base is a good platform for controlling electron configuration due to a facile synthesis of various organic structures (aldehyde or ketone groups with primary amine derivatives). The discussion focuses on the detection type, physicochemical and optical properties, and applications of these chemosensors.

Keywords: chemosensor; sensing; functional groups; Schiff base; fluorescence; colorimetric; metal ion



Citation: Park, J.-K.; Shin, J.; Jang, S.; Seol, M.-L.; Kang, J.; Choi, S.; Eom, H.; Kwon, O.; Park, S.; Noh, D.-Y.; et al. Rational Design of Fluorescent/Colorimetric Chemosensors for Detecting Transition Metal Ions by Varying Functional Groups. *Inorganics* **2022**, *10*, 189. <https://doi.org/10.3390/inorganics10110189>

Academic Editors:

Mireille Vonlanthen,

Fabián Cuétara-Guadarrama and

Ernesto Rivera

Received: 19 September 2022

Accepted: 26 October 2022

Published: 29 October 2022

Publisher's Note: MDPI stays neutral with regard to jurisdictional claims in published maps and institutional affiliations.



Copyright: © 2022 by the authors. Licensee MDPI, Basel, Switzerland. This article is an open access article distributed under the terms and conditions of the Creative Commons Attribution (CC BY) license (<https://creativecommons.org/licenses/by/4.0/>).

1. Introduction

The development of new chemicals has allowed us to better human life over the years. On the other hand, chemicals containing metallic materials were released randomly into the environment, and now they have accelerated the destruction of the environment and biological systems [1]. For example, mercury can cause damage to the human body such as respiratory, gastrointestinal, and central nervous system, which may result in diseases such as deafness, Minamata, and Alzheimer's [2–4]. Additionally, high concentrations of copper in the human body may cause ischemic heart disease, anemia, and neurological diseases such as Menkes and Alzheimer's [5–12]. Therefore, detecting the micromolar changes of metal ions is essential in complex media such as biological tissues and environmental samples. In this regard, chemosensors are considered the best candidates due to their great sensitivity and selectivity, fast response time, real-time detection capability, and low cost [13–16]. Depending on the signal transduction mechanism, they can be classified into colorimetric or fluorescent chemosensors.

Colorimetric chemosensors transform chemical information into color signals, which are visible to the naked eye. In general, π -conjugated molecules with a small energy gap between the highest energy occupied molecular orbital (HOMO) and the lowest energy unoccupied molecular orbital (LUMO) have been used as colorimetric sensing materials because they absorb long-wavelength light and emit visible light (380–700 nm).

The sensing material recognizes metal ions through chemical interactions that regulate the sensor bandgap. For instance, decreasing the HOMO–LUMO energy gap results in a bathochromic (red) shift, while increasing it leads to a hypsochromic (blue) shift [14]. When electron-donating and -withdrawing groups are introduced into this conjugated system, intramolecular electron transfer occurs, affecting the photophysical properties of the sensor [17].

Fluorescent chemosensors produce a luminescence signal under ultraviolet (UV) light and offer advantages including low limit of detection (LOD), reversibility, and wide applicability. Their basic operation relies on the emission of light irradiation when the excited state of the electrons relaxes to the ground state. Fluorescent chemosensors consist of a series of signaling fluorophores and recognition chemical moieties. The existence of analyte generates changes in the physicochemical properties of sensor as the analyte binds to the recognition moiety, which leads to conversion of information to fluorescence by the signaling fluorophore [1,14,16,18]. The results of sensing assay can be explained by two fluorescence effects: chelation-enhanced fluorescence (CHEF) of turn-on mode and chelation-quenched fluorescence (CHEQ) of turn-off mode [18–20]. Both effects are related to multiple signaling mechanisms involving electron transfer.

The abovementioned colorimetric absorption spectra and fluorescence emission are attributed to electron transfer mechanisms such as internal charge transfer (ICT) [15,19–25], photoinduced electron transfer (PET) [15,19–26], metal-to-ligand charge transfer (MLCT) [19,21,23,27], and C = N isomerization [19,28]. In design of a chemosensor, a promising strategy for controlling the electron transfer mechanism is in coordination of the functional groups, which can modify the electron distributions and spectroscopic properties [16,29–31]; furthermore, functional groups can enhance the receptor affinity to the metal ions by varying its electron density for stronger interact with those sensing target. Depending on the functional groups, the target metal ions can also be selectively detected in solutions even with interfering ions [32–34].

Following the advantages of controlling the functional groups for high-performance chemosensors, numerous Schiff bases have been designed as sensors to utilize their applicability to diverse functional groups, facile synthesis, and possibility of detecting assorted metal ions [20,35–38]. A Schiff base can be easily synthesized by condensing any aldehyde or ketone with primary amine derivatives. Using the various types of amine derivatives, electron configuration of sensing material can be tuned, ultimately affecting to sensing ability. Moreover, the C = N ligand in Schiff base acts as hard-base donor sites and this enhances selective reactivity [35,39–43]. For these reasons and their high-intensity emission after binding with metal ions, Schiff bases have been used considerably as chemosensors.

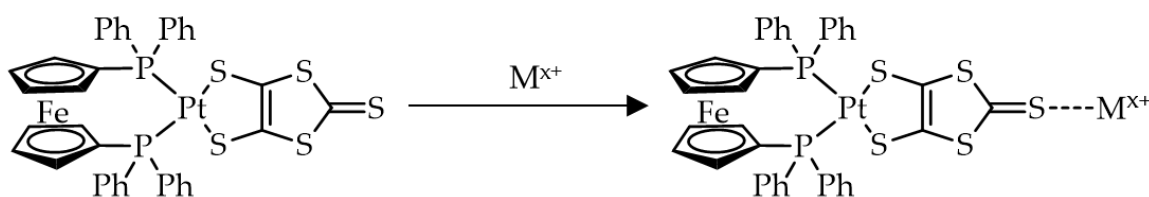
This review focuses mainly on the various performances and detectable metal ions of chemosensors when functional groups are substituted. Pt(dithiolene)-based chemosensors are discussed to show how the electron-donating functional groups affect to the sensor performance. Then, recent examples of Schiff base chemosensors (2014–2021) with thiophene, julolidine, and rhodamine moieties are discussed specifically for their excellent photophysical properties including high absorptivity, good thermal stability and photostability, good quantum yield, and ease of structural manipulation to adjust the electronic and optical properties. At the end, the main capabilities and applications of each sensing molecule are summarized.

2. Pt(dithiolene)-Based Chemosensors

This section discusses sensing materials based on (diphosphine)Pt(dmit) complexes (dmit: 1,3-dithiole2-thione-4,5-dithiolate). The thione moiety in the dmit ligand serves as the analyte-detecting site; it contains both π -electrons on the C = S bond and lone pair electrons on the S atom. The metal ions coordinate with the thione moiety through $\pi \rightarrow \pi^*$ transitions, transducing the chemical signals into color variations. These sensing materials show different photophysical properties depending on the substitution of their different types of functional groups, which are denoted as dxpe ($x = p$ (phenyl)),

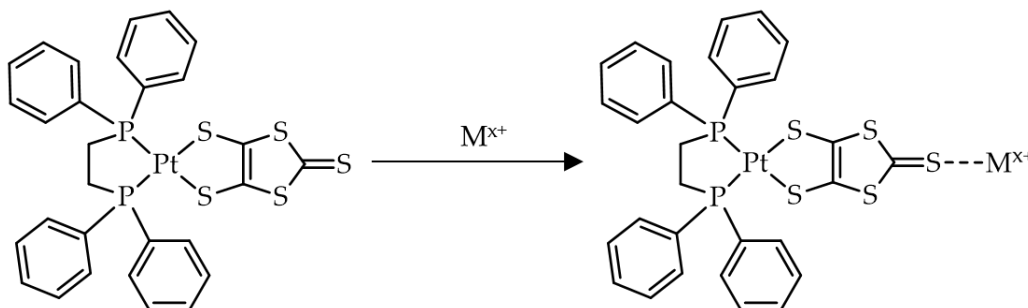
fp (pentafluorophenyl), and ch (cyclohexyl)) in (dxpe)Pt(dmit). When strong electron-donating functional groups such as cyclohexyl substitutes the diphosphine ligand, the resulting sensor can detect a wide range of metal ions (Ag^+ , Cu^{2+} , Hg^{2+}). This indicates that modulation of the electronic structures affects the selectivity, sensitivity, number of detectable metal ions, and multiple-ion detection ability in the co-existence of interfering ions in media.

(dppf)Pt(dmit) (**1**) (dppf: 1,1'-bis(diphenylphosphino)ferrocene) (Scheme 1) is an effective probe for Hg^{2+} ions in solution. The absorption spectrum of **1**- Hg^{2+} shows a bathochromic shift to 537 nm that originates from the $\pi \rightarrow \pi^*$ transition of the $\text{C}=\text{S}$ moiety in the dmit ligand, with a color change from yellow to purple. The stoichiometric ratio between **1** and Hg^{2+} is 1:1 [32].

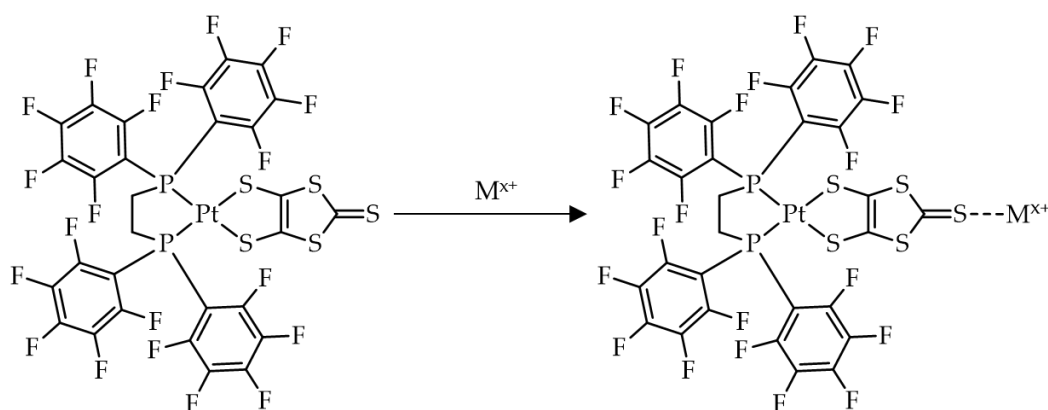


Scheme 1. Chemosensor (1,1'-bis(diphenylphosphino)ferrocene)Pt(1,3-dithiole2-thione-4,5-dithiolate) (**1**) and its complex with the target metal ion.

(dppe)Pt(dmit) (**2**) (dppe: 1,2-bis(diphenylphosphino)ethylene) (Scheme 2) has good selective reactivity toward Hg^{2+} , Cu^{2+} and lower sensitivity to Ag^+ . According to the Job's plot, the binding ratio between **2** and heavy metal ions is 1:0.4. However, switching of the diphosphine end-group from dppe to dfppe (1,2-bis[bis(pentafluorophenyl)phosphino]ethane), yielding (dfppe)Pt(dmit) (**3**) (Scheme 3), dramatically influences the selectivity to metal ions [44].



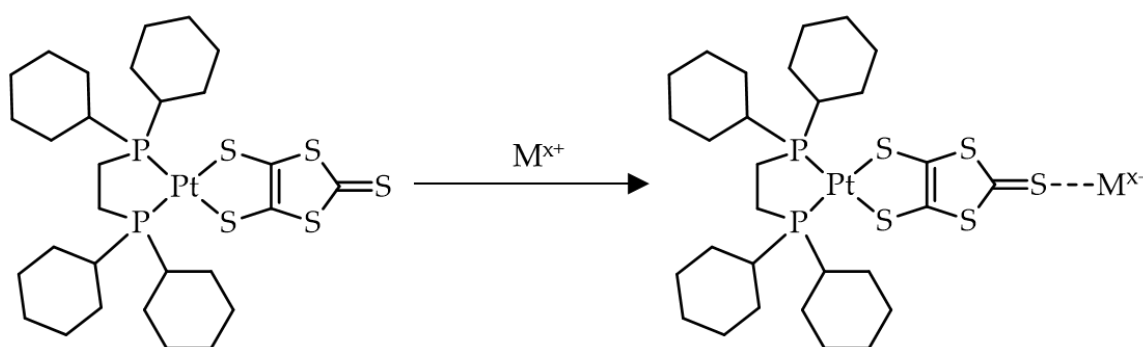
Scheme 2. Chemosensor (1,2-bis(diphenylphosphino)ethylene)Pt(1,3-dithiole2-thione-4,5-dithiolate) (**2**) and its complex with the target metal ion.



Scheme 3. Chemosensor (1,2-bis[bis(pentafluorophenyl)phosphino]ethane)Pt(1,3-dithiole2-thione-4,5-dithiolate) (**3**) and its complex with the target metal ion.

Sensing material **3** has a pentafluorophenyl functional group at the ligand end that induces hybridization shielding effect, allowing Hg^{2+} to be selectively detected among multiple metal ions. UV-vis spectroscopy analysis has shown three bathochromic shifts at 558, 700–800, and 530 nm as **2** interacts with Hg^{2+} , Cu^{2+} , and Ag^+ , respectively. However, the absorption peak of **3** exhibits a different behavior: only a bathochromic shift at 523 nm due to interactions with Hg^{2+} . The same tendency is observed in the color changes; the color of the **3** aqueous solution changes only in the presence of Hg^{2+} , from yellow to vivid red, while the **2** aqueous solution undergoes three weak color changes in the presence of Hg^{2+} , Cu^{2+} , and Ag^+ . Density functional theory (DFT) calculations have been conducted to investigate the interacting mechanism of **2** and **3** with cations, revealing different electronegativities due to hydrogen and fluorine in their diphosphine ligands. As a result, the level of electronic hybridization between **3** and Hg^{2+} is remarkably higher than that with other ions [33].

(dchpe)Pt(dmit) **4** (dchpe: 1,2-bis(dicyclohexylphosphino)ethane) (Scheme 4) has cyclohexyl groups in the diphosphine ligand. These cyclohexyl groups increase the electron density of the thione moiety, allowing Hg^{2+} , Cu^{2+} , and Ag^+ to be detected in a solution even with coexisting other interfering metal ions. Its absorption peak exhibits a hypsochromic shift at 578 nm for Hg^{2+} , 700–800 nm for Cu^{2+} , and 472 nm for Ag^+ because the high electron-donating ability of the cyclohexyl groups de-shields the dmit ligand. As a result, the solution changes its color from yellow to deep navy, orange, and yellow in response to Hg^{2+} , Cu^{2+} , and Ag^+ , respectively. The stoichiometric binding ratio between **4** and Hg^{2+} is 1:1 according to the Job's plot analysis. DFT calculation data support strong binding affinity to Hg^{2+} , Cu^{2+} , and Ag^+ ; thereby, **4** showed high selectivity without interference of other metal ions [34].



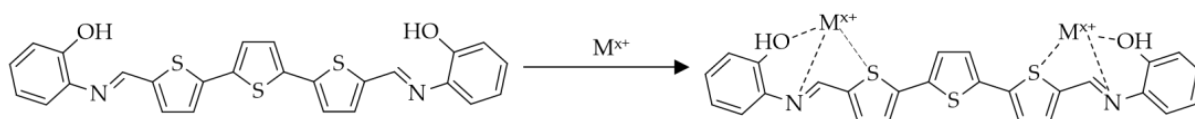
Scheme 4. Chemosensor (1,2-bis(dicyclohexylphosphino)ethane)Pt(1,3-dithiole2-thione-4,5-dithiolate) (**4**) and its complex with the target metal ion.

3. Thiophene-Based Chemosensors

Thiophene-based chemosensors are broadly used as light-emitting materials for selective detection of metal ions due to their easy synthesis, cost-effectiveness, extended emission and absorption wavelengths, and vast absorption. Thiophene-based Schiff bases can be prepared as chemosensors by the reaction between aldehyde- or ketone-group-containing thiophene derivatives with primary amines.

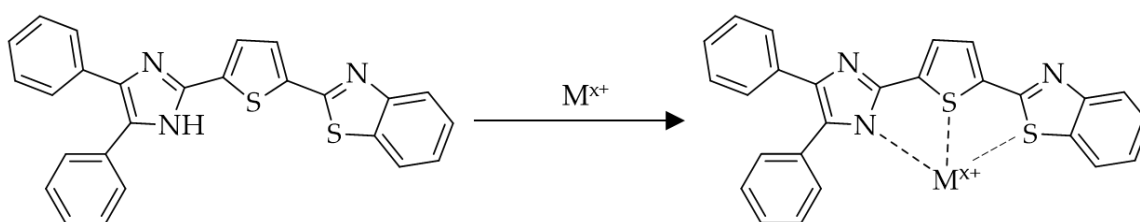
The dual-mode fluorescent chemosensor **5** (Scheme 5) is synthesized by the reaction of amine derivative 2-aminophenol with [2,2':5',2''-terthiophene]-5,5''-dicarbaldehyde. It can detect Fe^{3+} and Hg^{2+} by the CHEF effect, and has both colorimetric and fluorescent properties. Upon interaction with Fe^{3+} or Hg^{2+} , its fluorescence emission peak is enhanced from 360 to 520 nm. The fluorescence intensity of the **5**–metal ion complex is not changed in a wide range of pH (4.0–12.0). Moreover, the color of the **5** solution changes from khaki to reddish brown due to the formation of the **5**– Hg^{2+} complex, with an absorption peak shift from 360 to 415 nm. The LOD of **5** for Fe^{3+} and Hg^{2+} in aqueous solution are, 3.52×10^{-8} and 5.0×10^{-8} M, respectively, while the binding ratio between **5** and $\text{Fe}^{3+}/\text{Hg}^{2+}$ is 1:2. The **5** has been tested also in river water, tap water, and distilled water for its practical

feasibility, and the results satisfy the recommended guidelines. A reversibility test has demonstrated that the 5-Hg²⁺ complex can be recovered but not for 5-Fe³⁺ one [45].



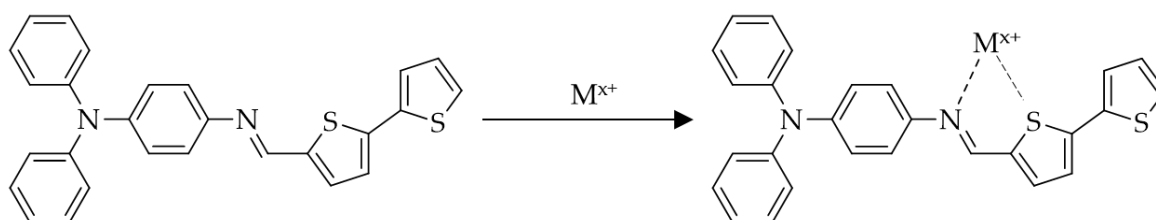
Scheme 5. Chemosensor 5 2,2'-(((1*E*,1'*E*)-[2,2':5',2''-terthiophene]-5,5''-diylbis(methaneylylidene)) bis(azanylylidene))diphenol and its complex with the target metal ion.

The fluorescence turn-on sensing material 6 (Scheme 6) is obtained by bridging imidazole and benzothiazole moieties through a thiophene ring. Upon interaction with Hg²⁺, its emission intensity shows a blue shift with slightly decrease in fluorescence intensity by the CHEF mechanism, and, correspondingly, its fluorescent green color turns into blue. However, 6 is non-fluorescent upon interaction with Cu²⁺, indicating significant decrease in fluorescence intensity by the CHEQ effect after the MLCT reaction. Both 6-Hg²⁺ and 6-Cu²⁺ complexes have a binding ratio of 1:1, and the corresponding LOD are 28 and 7.5 nM, respectively; these complexes do not interfere with each other, indicating great selectivity. Moreover, 6 provides outstanding cell permeability and high sensitivity toward Hg²⁺ and Cu²⁺ for the application to biological and environmental systems [46].



Scheme 6. Chemosensor 6 2-(5-(4,5-diphenyl-1*H*-imidazol-2-yl)thiophen-2-yl)benzo[*d*]thiazole and its complex with the target metal ion.

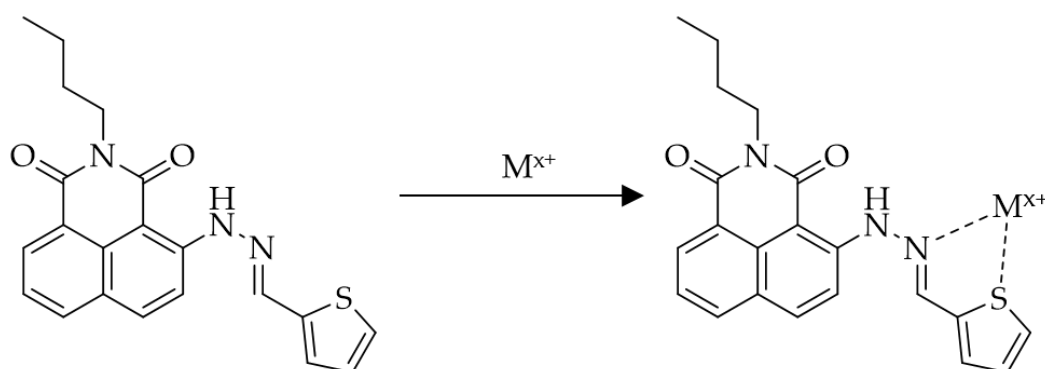
The sensing material 7 (Scheme 7) is synthesized from 4-nitro-triphenylamine, 4-amino-triphenylamine, and 2,2'-bithiophene-5-carboxaldehyde, and it possesses good optoelectronic properties. After the addition of Cr³⁺, Saxon blue color becomes dominant in the 7-Cr³⁺ solution under UV light (366 nm) by the PET process. Moreover, the fluorescence intensity increases until the pH reaches 7, and then decreases due to the formation of chromium hydroxide, which inhibits the formation of 7-Cr³⁺, at higher pH values. Further studies have revealed that the fluorescence signal is maintained up to 3600 s and the quantum yield of 7 is 28%. The fluorescence intensity gradually increases in the range between 1.25×10^{-4} and 6.25×10^{-6} M, and the binding ratio between 7 and Cr³⁺ is 2:1 according to the Job's plot analysis. Furthermore, the LOD of 7 for Cr³⁺ is 1.5 μ M and highly reversible [47].



Scheme 7. Chemosensor 7 (*E*)-4-((2,2'-bithiophen]-5-ylmethylene)amino)-*N,N*-diphenylamine and its complex with the target metal ion.

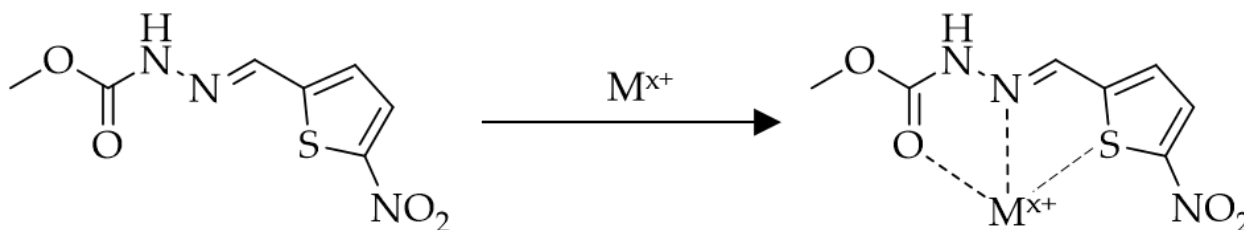
The fluorescence sensing material 8 (Scheme 8) is synthesized through a reaction between 6-hydrazino-benzo[*de*]isoquinoline-1,3-dione and 2-thiophene formaldehyde. Sensing material 8 in a CH₃CN/hydroxyethyl piperazine ethane sulfonic acid (HEPES)

(3:2, *v/v*) solution has been prepared to examine its UV–Vis absorption. Upon Cu^{2+} addition to the solution, the absorption intensity at ~ 465 nm has been selectively decreased. Sensing material **8** has a strong fluorescence emission at 575 nm, whose intensity gradually decreases when adding Cu^{2+} due to its strong binding interaction with the thiophene moiety. Moreover, **8** has a relatively stable structure in a broad pH range. According to the Job's plot, the stoichiometric ratio between **8** and Cu^{2+} is 1:1. The association constant is $7.8 \times 10^5 \text{ M}^{-1}$ and the LOD for Cu^{2+} is 1.8 μM . Moreover, **8** exhibits irreversible features when EDTA is added to the **8**– Cu^{2+} solution, indicating no meaningful recovery for the fluorescent intensity. The cell fluorescence imaging capacity of **8** has been examined in living cells, resulting in significant intracellular green fluorescence, which demonstrates its usefulness in environmental and biological systems [48].



Scheme 8. Chemosensor **8** (*E*)-2-butyl-4-(2-(thiophen-2-ylmethylene)hydrazineyl)-1*H*-benzo[*de*]isoquinoline-1,3(2*H*)-dione and its complex with the target metal ion.

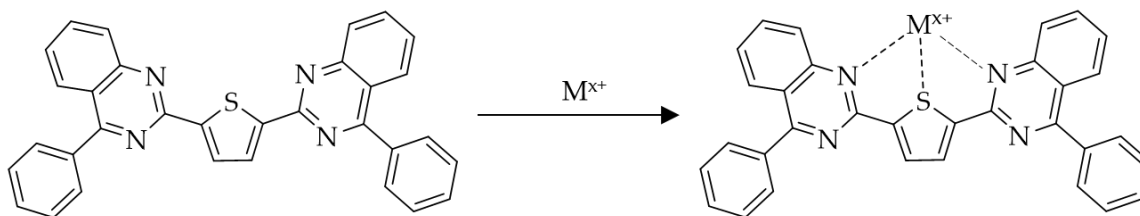
The sensing material **9** (Scheme 9) is synthesized to detect Ag^+ in aqueous media with a fluorescence blue shift due to its oxygen, sulfur, and nitrogen atoms. When Ag^+ coordinates with **9**, a significant hypsochromic shift occurs from 425 to 405 nm due to the ICT mechanism. Based on the Job's plot and mass spectrum, the stoichiometric ratio between **9** and Ag^+ is 1:1. Furthermore, the LOD for Ag^+ is $1.28 \times 10^{-7} \text{ M}$ and the association constant is $1.58 \times 10^6 \text{ M}^{-1}$. Sensing material **9** is stable in a wide range of pH (4.0–9.0). To investigate its practical usage in biology, *Escherichia coli* cells have been analyzed in the absence or presence of Ag^+ . In the presence of Ag^+ , **9** has shown a high red fluorescence intensity inside the cells, proving its applicability as a chemosensor for Ag^+ in live cells; **9** could also be potentially utilized in real water, paving the way for both biological and aqueous environment applications [49].



Scheme 9. Chemosensor **9** methyl (*E*)-2-((5-nitrothiophen-2-yl)methylene)hydrazine-1-carboxylate and its complex with the target metal ion.

The Thiophene-based sensing material **10** (Scheme 10) can selectively detect Fe^{3+} . Its absorption and fluorescence spectra have been measured in a CH_3CN solution. Upon its interaction with Fe^{3+} , the UV–Vis absorption peak shows a fluorescence bathochromic shift to 533 nm, which could be attributed to ICT process between thiophene and phenylquinazoline; correspondingly, in the presence of Fe^{3+} , the color changes from colorless to greenish-yellow, with the appearance of predominant absorption peak at 419 nm. Based on the

results of matrix-assisted laser desorption/ionization time-of-flight analysis and the Job's plot, the stoichiometric binding ratio of **10**-Fe³⁺ is 1:1. The LOD is 1.6×10^{-8} M, indicating good sensitivity for Fe³⁺. Upon addition of EDTA to the **10**-Fe³⁺ solution, the complex is dissociated and an absorption peak similar to **10** is observed, indicating the sensor reversibility. In terms of practical applications, this reversibility and the fluorescence emission could allow the use of **10** as a molecular logic gate [50].

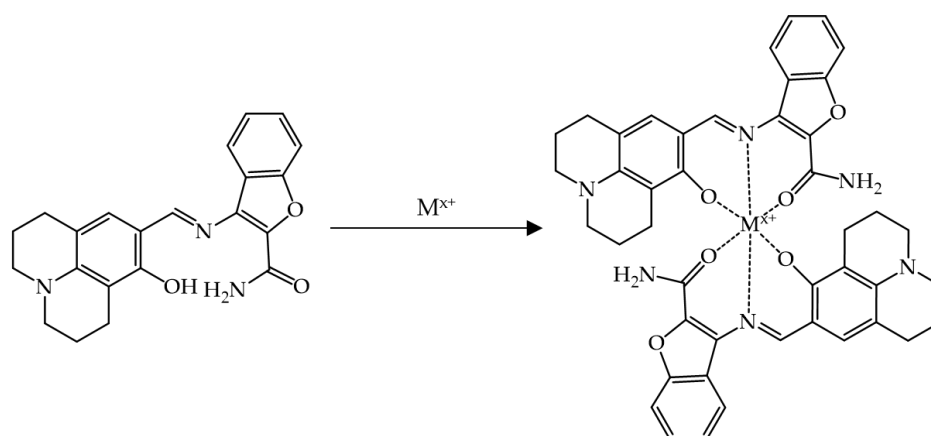


Scheme 10. Chemosensor **10** 2,5-bis(4-phenylquinazolin-2-yl)thiophene and its complex with the target metal ion.

4. Julolidine-Based Chemosensors

The julolidine moiety is water-soluble and a well-known chromophore and fluorophore that has been used in colorimetric and fluorescent sensors. For the synthesis of julolidine-based Schiff bases as chemosensors, 8-hydroxy julolidine-9-carboxaldehyde is used as the starting material to obtain Schiff base, and various types of amine derivatives are selected to provide different sensing properties.

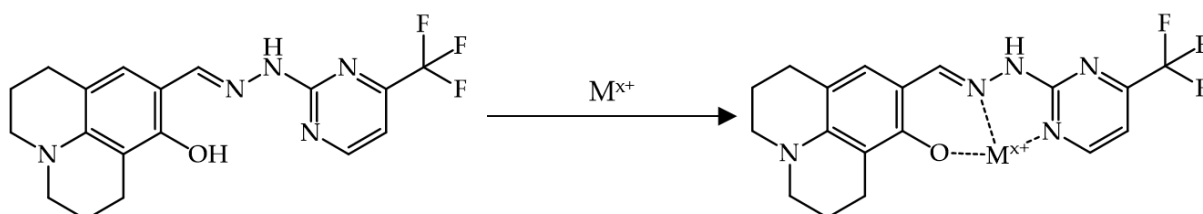
The sensing material **11** (Scheme 11) is prepared using 3-aminobenzofuran-2-carboxamide as the amine source. It can effectively detect Fe³⁺ and Fe²⁺ by observing a color change from yellow to brown in a near-perfect aqueous environment. The formation of the iron complex is revealed by a clear isosbestic point at 382 (Fe³⁺, Fe²⁺) and 468 nm (Fe²⁺) in the UV-Vis spectra. The color change of the solution is caused by the MLCT mechanism. The binding stoichiometry of **11** with the iron ions is 2:1; the LOD is 0.36 μ M for Fe³⁺ and 0.37 μ M for Fe²⁺, much lower than the guideline of iron in drinking water (5.37 μ M) set by the Environmental Protection Agency (EPA). Moreover, a competitive study has shown that there is no significant interference in the detection of iron ions, indicating selective reactivity with Fe³⁺ and Fe²⁺ [51].



Scheme 11. Chemosensor **11** (*E*)-3-(((8-hydroxy-2,3,6,7-tetrahydro-1*H*,5*H*-pyrido[3,2,1-*ij*]quinolin-9-yl)methylene)amino)benzofuran-2-carboxamide and its complex with the target metal ion.

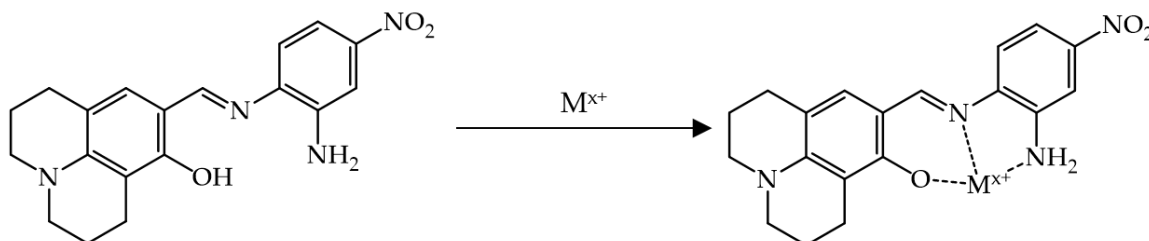
The sensing material **12** (Scheme 12) is derived from 2-hydrazinyl-4-(trifluoromethyl)pyrimidine. It possesses high selectivity and sensitivity to Cu²⁺ and Co²⁺ in aqueous solutions and can be used to detect both ions in real water samples. It exhibits the maximum absorption band centered at 375 nm, then it shows a bathochromic shift upon binding to Cu²⁺ and Co²⁺. This leads to a change in color from transparent to light yellow. Based

on the Job's plot, the binding stoichiometry between **12** and the target metal ions is 1:1. Inhibition experiments have shown that the detection ability of **12** to Cu^{2+} and Cu^{2+} is hardly affected by coexisting competitive ions. Moreover, the LOD for Cu^{2+} (0.19 μM) and Co^{2+} (0.18 μM) of **12** are significantly lower than the World Health Organization (WHO) guideline for Cu^{2+} (31.5 μM) and the EPA guideline for Co^{2+} (17 μM). The pH range of 6.0–10.0 and the high recovery value of tap water and drinking water demonstrate its practical applicability [52].



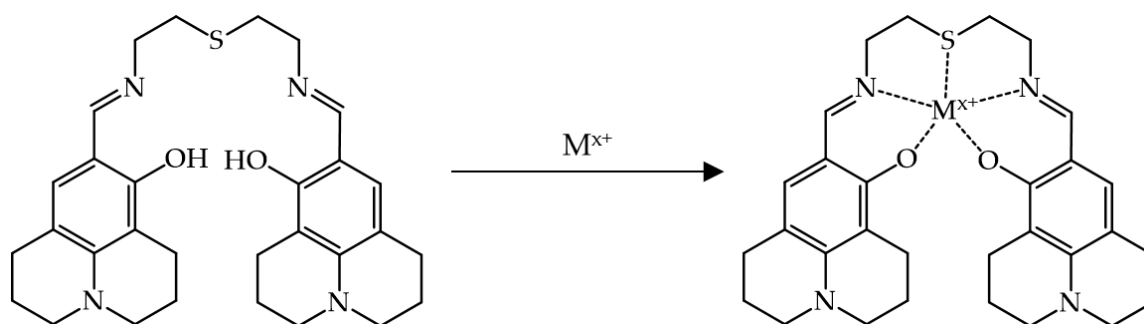
Scheme 12. Chemosensor **12** (*E*)-9-((2-(4-(trifluoromethyl)pyrimidin-2-yl)hydrazineylidene)methyl)-2,3,6,7-tetrahydro-1*H*,5*H*-pyrido[3,2,1-*ij*]quinolin-8-ol and its complex with the target metal ion.

The sensing material **13** (Scheme 13) is obtained by the condensation reaction of 4-nitro-1,2-phenylenediamine reactants and is utilized as a colorimetric chemosensor of Cu^{2+} . A bathochromic shift indicates ICT between Cu^{2+} and the electron-withdrawing groups, such as the $\text{C} = \text{N}$ group, in **13**; this, in turn, changes the color from pale yellow to orange in aqueous solutions. Moreover, its large molar extinction coefficient ($6.3 \times 10^3 \text{ M}^{-1} \text{ cm}^{-1}$) proves that the binding mechanism corresponds to MLCT. The **13**– Cu^{2+} complex has a 1:1 stoichiometry ratio and the LOD for Cu^{2+} is 0.37 μM . Competitive experiments have shown that **13** has selective reactivity with Cu^{2+} in the presence of various metal ions. The absorbance spectra study of **13**– Cu^{2+} complexes with various amino acids and peptides indicates that of **13** is applicable as a colorimetric chemosensor for cysteine and histidine in aqueous media as well [53].



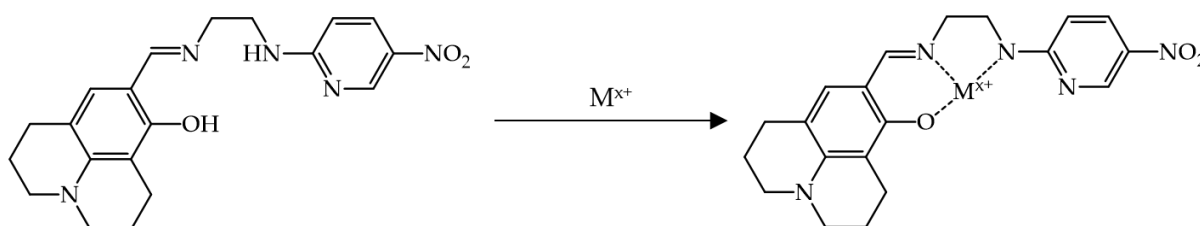
Scheme 13. Chemosensor **13** (*E*)-9-(((2-amino-4-nitrophenyl)imino)methyl)-2,3,6,7-tetrahydro-1*H*,5*H*-pyrido[3,2,1-*ij*]quinolin-8-ol and its complex with the target metal ion.

The material **14** (Scheme 14) can serve as a fluorescent sensor for Zn^{2+} and Al^{3+} and as a colorimetric sensor for Fe^{2+} or Fe^{3+} . In its synthesis, 2,2'-thiobis-(ethylamine) is used as an amine derivative. The addition of Zn^{2+} or Al^{3+} enhanced the emission intensity at 448 or 418 nm, respectively, which is induced by the inhibition of $\text{C} = \text{N}$ isomerization and excited-state proton transfer. Moreover, the chelation of **14**– Zn^{2+} or **14**– Al^{3+} results in rigid complexes, leading to a significant CHEF effect. The **14**– Zn^{2+} and **14**– Al^{3+} complexes have a 1:1 complexation stoichiometry, and the corresponding LOD of 1.59 and 1.34 μM , respectively. Additionally, **14** exhibits selective reactivity with Zn^{2+} in the presence of other metal ions. Furthermore, its chromogenic sensing ability toward Fe^{2+} and Fe^{3+} is expressed by a clear color change from yellow to dark green in aqueous solutions by MLCT. The complexation stoichiometry between **14** and Fe^{2+} or Fe^{3+} is 1:1, with a corresponding LOD of 0.21 or 0.22 μM , respectively. Fe^{3+} detection tests have shown high recovery (>96%) for tap water and deionized water samples [54].



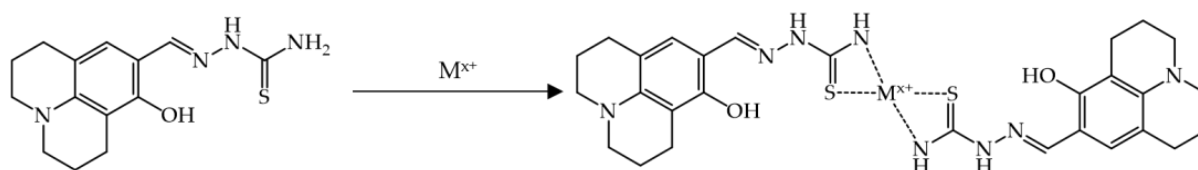
Scheme 14. Chemosensor **14** 9,9'-((1*E*,1'*E*)-((thiobis(ethane-2,1-diyl))bis(azanylylidene))bis(methaneylylidene))bis(2,3,6,7-tetrahydro-1*H*,5*H*-pyrido[3,2,1-*ij*]quinolin-8-ol) and its complex with the target metal ion.

The sensing material **15** (Scheme 15) is obtained from *N*-(2-aminoethyl)-5-nitropyridin-2-amine and is used as a colorimetric chemosensor to selectively detect Cu^{2+} . The addition of Cu^{2+} into a **15** solution results in enhanced absorbance at 450 nm. It enables an immediate color change from colorless to yellow; the new peak at 450 nm is attributed to an LMCT phenomenon. The **15**– Cu^{2+} complex was formed with a 1:1 stoichiometry ratio, and the corresponding LOD (23.5 μM) is lower than the safety standard for drinking water. The sensor **15** shows colorimetric responses in the presence of Cu^{2+} over wide range of pH (7–12), indicating excellent practical applicability. Upon the addition of EDTA to the **15**– Cu^{2+} solution, the complex is dissociated, and the color changed from yellow to colorless, indicating that the sensor **15** is chemically reversible [55].



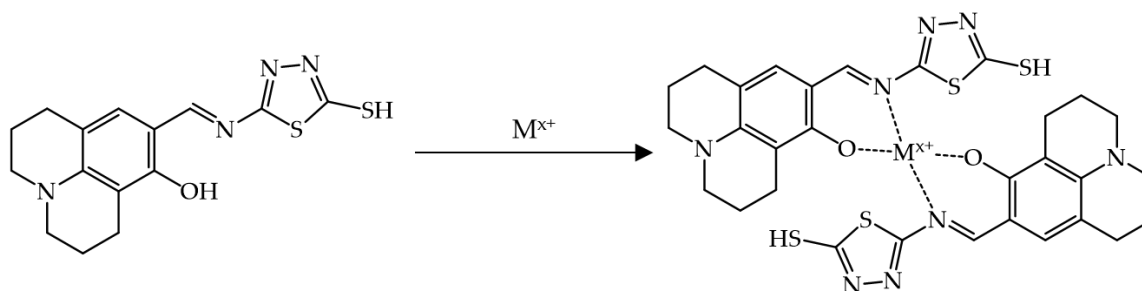
Scheme 15. Chemosensor **15** (*E*)-9-(((2-((5-nitropyridin-2-yl)amino)ethyl)imino)methyl)-2,3,6,7-tetrahydro-1*H*,5*H*-pyrido[3,2,1-*ij*]quinolin-8-ol and its complex with the target metal ion.

The sensing material **16** (Scheme 16) is synthesized by the combination of thiosemicarbazide and julolidine moiety. It exhibits an ON–OFF of fluorescence in response to Hg^{2+} , involves drastic decrease in the emission intensity at 453 nm. The binding ratio of the **16**– Hg^{2+} complex is 1:2 with the intramolecular interaction between Hg^{2+} and OH (in the julolidine moiety) or NH_2 (in the thiosemicarbazide moiety) functional groups. Sensing material **16** can sensitively detect Hg^{2+} with an LOD of 0.59 μM and shows excellent selective reactivity in the presence of other metal ions. Selectivity tests with various amino acids and peptides have demonstrated that the **16**– Hg^{2+} complex can be successfully utilized with thiol-containing cysteine or glutathione [56].



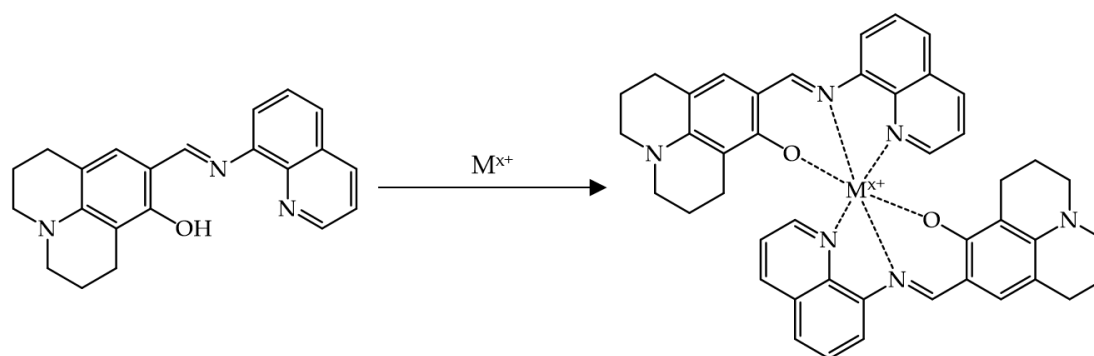
Scheme 16. Chemosensor **16** (*E*)-2-((8-hydroxy-2,3,6,7-tetrahydro-1*H*,5*H*-pyrido[3,2,1-*ij*]quinolin-9-yl)methylene)hydrazine-1-carbothioamide and its complex with the target metal ion.

The material **17** (Scheme 17) is designed as a colorimetric chemosensor for Cu^{2+} and is prepared using 5-amino-1,3,4-thiadiazole-2-thiol amine derivatives. Upon addition of Cu^{2+} , a peak at 450 nm decreased, while a new band at 525 nm gradually increased in the UV-vis spectrum, leading changes in color from yellow to orange. Due to the large molar extinction coefficient, the color change can be explained by the LMCT mechanism. The **17**- Cu^{2+} complex has a 1:2 binding ratio with an excellent corresponding LOD (0.9 μM). Moreover, **17** showed selective reactivity toward Cu^{2+} in the presence of other metal ions. Sensing material **17** has been tested also in tap water and distilled water to prove its practical feasibility, and satisfactory repeatability and reproducibility were verified [57].



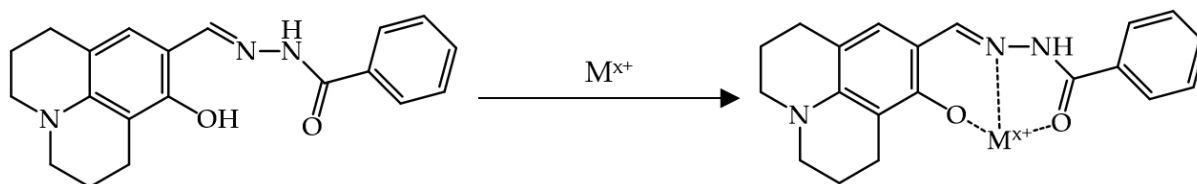
Scheme 17. Chemosensor **17** (*E*)-9-(((5-mercapto-1,3,4-thiadiazol-2-yl)imino)methyl)-2,3,6,7-tetrahydro-1*H*,5*H*-pyrido[3,2,1-*ij*]quinolin-8-ol and its complex with the target metal ion.

The sensing material **18** (Scheme 18) is obtained by condensation reaction with quinoline-8-amine reactants. It has been proposed as a colorimetric chemosensor to selectively detect Co^{2+} . The addition of Co^{2+} to the **18** solution changes the color from yellow to orange by forming an **18**- Co^{2+} complex with a 2:1 stoichiometry ratio. For Co^{2+} , **18** shows a excellent LOD (1.28×10^{-6} M) which is lower than the recommended safety guideline. Furthermore, **18** possesses good selectivity for Co^{2+} in the presence of various competing metal ions. The sensor **18** shows colorimetric responses in the presence of Co^{2+} at wide range of pH (4–11), proving its practicality [58].



Scheme 18. Chemosensor **18** (*E*)-9-((quinolin-8-ylimino)methyl)-2,3,6,7-tetrahydro-1*H*,5*H*-pyrido[3,2,1-*ij*]quinolin-8-ol and its complex with the target metal ion.

The sensing material **19** (Scheme 19) is synthesized via coupling reaction with benzhydrazide amine derivatives. It exhibited selective fluorescence sensing ability for Al^{3+} . The interaction between **19** and Al^{3+} results in enhanced fluorescence intensity with a high quantum yield of 0.502, which can rely on excited-state intramolecular proton transfer, C = N isomerization, and the CHEF effect. Sensing material **19** and Al^{3+} form a complex with a 1:1 binding ratio; the LOD is 0.193 μM , much lower than the WHO guideline for drinking water. Competitive experiments have revealed selective reactivity with Al^{3+} in the presence of other interfering metal ions, except for Fe^{2+} , Fe^{3+} , Cu^{2+} , and Cr^{3+} . Moreover, tests with human dermal fibroblasts have demonstrated the efficiency of **19** for Al^{3+} imaging in live cells [59].

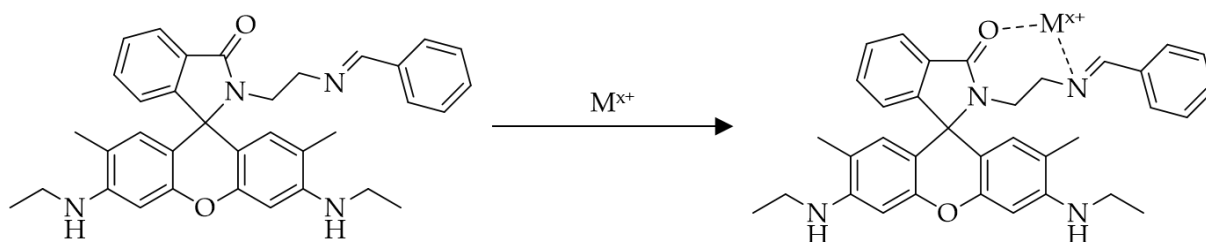


Scheme 19. Chemosensor **19** (*E*)-*N'*-((8-hydroxy-2,3,6,7-tetrahydro-1*H*,5*H*-pyrido[3,2,1-*ij*]quinolin-9-yl)methylene)benzohydrazide and its complex with the target metal ion.

5. Rhodamine-Based Chemosensors

Rhodamine-based Schiff bases have attracted interest as both fluorescent and colorimetric chemosensors due to their excellent photophysical properties: high photostability, high quantum yield, good solubility, large molar absorption coefficient, and emission properties. Furthermore, since the rhodamine fluorophore has an emission wavelength of 550 nm or higher, the influence of background fluorescence (<500 nm) can be avoided, enabling highly sensitive detection. Rhodamine derivatives can be used as starting materials for these chemosensors and show different properties depending on their functional groups. The spirolactam moiety, frequently observed in rhodamine derivatives, has a five-membered ring moiety with non-fluorescent and colorless properties; however, the ring-opening reaction in the presence of a heavy metal atom gives rise to a change of absorbance and strong fluorescence emission. These characteristic changes in absorbance and fluorescence emission properties indicate its applicability as an ON–OFF fluorescent chemosensor.

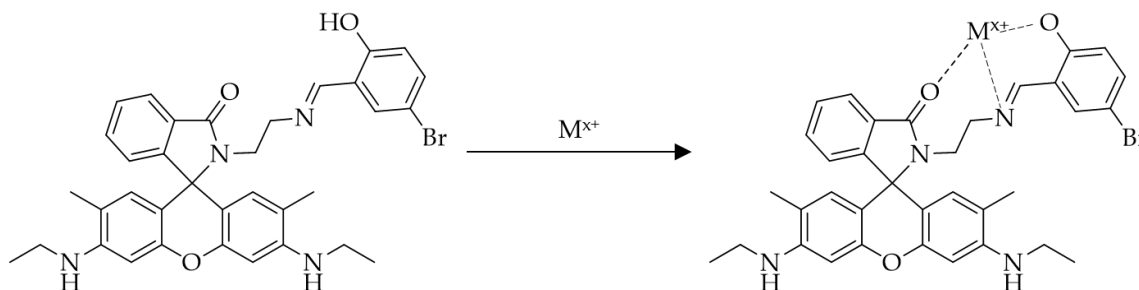
The sensing material **20** (Scheme 20) is synthesized by adding benzaldehyde into rhodamine ethylene diamine; it is used as a fluorescence chemosensor to selectively detect Fe^{3+} in biological systems. Proton nuclear magnetic resonance and electrospray ionization mass spectrometry analyses have revealed that the hydrolysis of the Schiff base (imine) and ring-opening of spirolactam affect the fluorescence emission. In the presence of Fe^{3+} , new absorption and emission bands appear at 526 and 551 nm. In the presence of biologically relevant metal ions such as Na^+ , K^+ , Ca^{2+} , Fe^{2+} , Mg^{2+} , and Mn^{2+} , the fluorescence intensities are negligibly changed, which indicates that **20** can be utilized for selective detection of Fe^{3+} . Its sensing ability toward Fe^{3+} in live cells has been evaluated using iron-overloaded human hepatoma cells; **20** has exhibited highly selectivity with Fe^{3+} , demonstrating its capability for Fe^{3+} imaging in biological environments [60].



Scheme 20. Chemosensor **20** (*E*)-2-(2-(benzylideneamino)ethyl)-3',6'-bis(ethylamino)-2',7'-dimethylspiro[isoinoline-1,9'-xanthen]-3-one and its complex with the target metal ion.

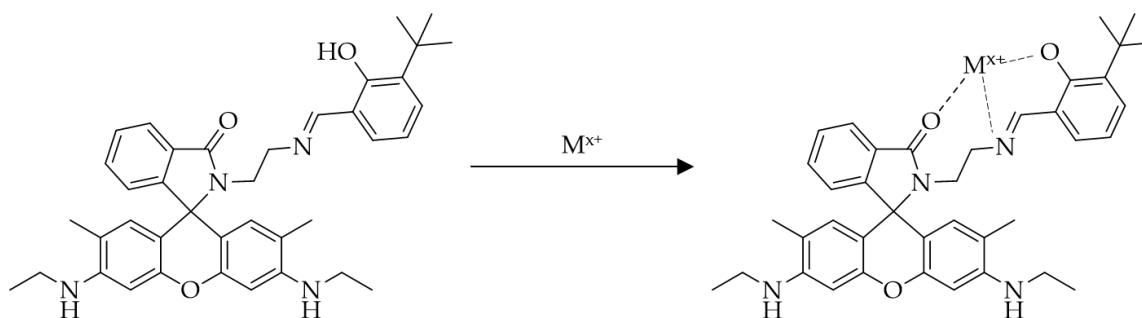
The sensing material **21** (Scheme 21) can be obtained by synthesizing Rhodamine 6G and ethylenediamine followed by Schiff base condensation with the same equivalent of 5-bromosalicylaldehyde in methanol. In the presence of trivalent ions such as Al^{3+} , Cr^{3+} , and Fe^{3+} , the colorless solution of **21** turns pink, showing a new absorption band at 528 nm; this is attributed to the activation of the amide group by ring-opening in the spirolactam moiety. Sensing material **21** is non-fluorescence but, in the presence of Al^{3+} , Cr^{3+} , and Fe^{3+} , its emission intensity increases with a quantum yield of 0.75, 0.36, and 0.26, respectively. The fluorescence intensity of **21**– Al^{3+} complexes is greatly enhanced compared to **21**– Cr^{3+} and **21**– Fe^{3+} complexes because of the large CHEF effect which is induced by oxophilic

nature and the high ionic potential of Al^{3+} . The Job's plot analysis indicates that **21** and metal ions have a 1:1 binding stoichiometry. The LOD for Al^{3+} (1.18 nM), Cr^{3+} (1.80 nM), and Fe^{3+} (4.04 nM) suggests that **21** is highly sensitive for these trivalent cations [61].



Scheme 21. Chemosensor **21** (*E*)-2-(2-((5-bromo-2-hydroxybenzylidene)amino)ethyl)-3',6'-bis(ethylamino)-2',7'-dimethylspiro[isoin-doline-1,9'-xanthen]-3-one and its complex with the target metal ion.

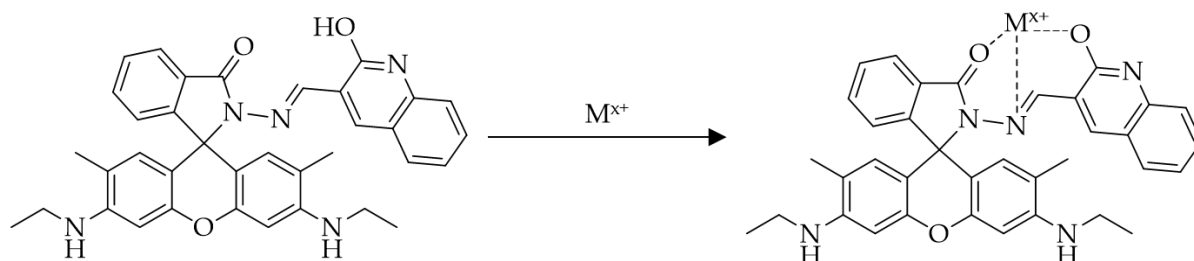
The sensing material **22** (Scheme 22) is composed of a rhodamine platform with a salicylaldehyde moiety. Upon the formation of the **22**- Al^{3+} or **22**- Zn^{2+} complex, a new absorption peaks appear at 528 or 375 nm. The new peak at 528 nm results from the ring-opening of the spiro-lactam structure attributed to Al^{3+} , while the peak at 375 nm is caused by the chelate formation between Zn^{2+} and **22**. Moreover, the fluorescence peak at 550 nm (or 457 nm) indicates that the addition of Al^{3+} (or Zn^{2+}) increases the fluorescence intensity as well. The quantum yield is 0.635 for 1 equiv. Al^{3+} and 0.508 for 1 equiv. Zn^{2+} . The LOD of **22** is 10.98 nM for Al^{3+} and 76.92 nM for Zn^{2+} . Under visible light, the Al^{3+} and Zn^{2+} solutions become yellow and blue, respectively, but only Al^{3+} exhibits a color change from colorless to yellow under UV irradiation [62].



Scheme 22. Chemosensor **22** (*E*)-2-(2-((3-(tert-butyl)-2-hydroxybenzylidene)amino)ethyl)-3',6'-bis(ethylamino)-2',7'-dimethylspiro[isoin-doline-1,9'-xanthen]-3-one and its complex with the target metal ion.

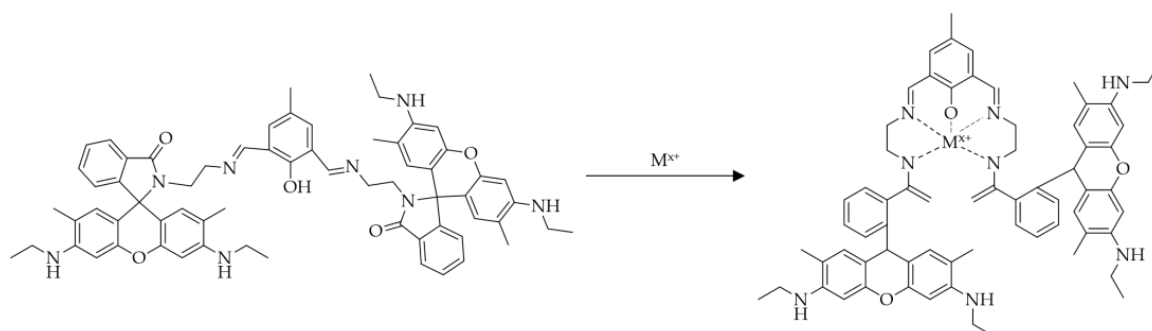
The sensing material **23** (Scheme 23) possesses high selectivity and sensitivity toward Fe^{3+} and Cu^{2+} . Sensing material **23** shows strong absorptions at 304 and 380 nm due to $\pi \rightarrow \pi^*$ and $n \rightarrow \pi^*$ transitions, respectively. In the range of 500–600 nm, however, it exhibits very small absorption and no fluorescence emission. The addition of Fe^{3+} and Cu^{2+} in its aqueous solution leads to the ring-opening process of the rhodamine moiety, resulting in a sharp and strong absorbance peak at 529 nm with a color change from colorless to pink. This chemosensor has low LOD for Fe^{3+} and Cu^{2+} (40 and 18 nM, respectively), and it has equimolar association ratio (1:1) with Fe^{3+} and Cu^{2+} according to the Job's plot. Sensing material **23** shows a remarkable enhancement of fluorescence at 572 nm in the presence of Fe^{3+} in an aqueous medium. It showed good linearity up to 250 μM and a low LOD (33 nM). The presence of Cu^{2+} , instead, does not induce any fluorescence emission. Some studies have experimented in various pH range (2.0–12.0) in phosphate-buffered saline solutions, revealing that increase in the acidity of the **23** solution enhances its absorbance

and fluorescence; this implies that the spirolactam ring is opened due to protonation of the lactam carbonyl. Moreover, **23** has a wide pH detection range for its target metal ions, and it could be adapted to detect Fe^{3+} in living cell animal models and zebrafish embryos [63].



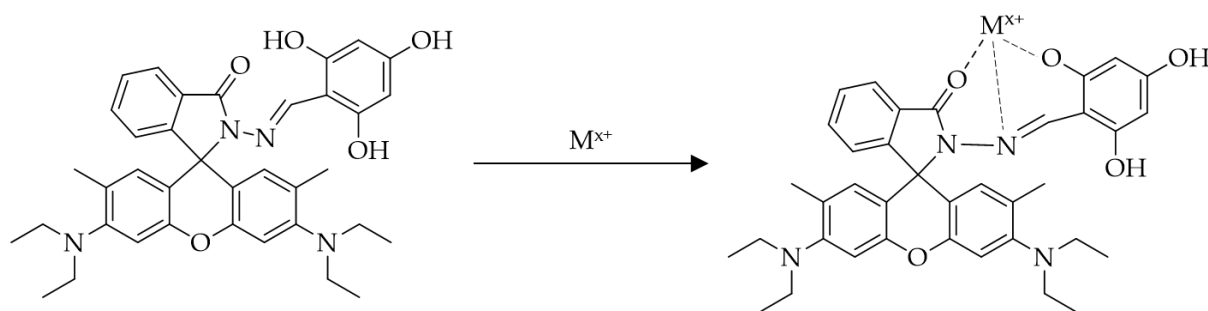
Scheme 23. Chemosensor **23** (*E*)-3',6'-bis(ethylamino)-2-(((2-hydroxyquinolin-3-yl)methylene)amino)-2',7'-dimethylspiro[isindoline-1,9'-xanthen]-3-one and its complex with the target metal ion.

The Rhodamine 6G-based sensing material **24** (Scheme 24) has a high affinity to Pb^{2+} in aqueous solutions. In the presence of Pb^{2+} , a strong absorption band is observed at 528 nm due to the increase in the acyclic xanthen form, and the solution color correspondingly changes from light yellow to pink. Further fluorescent titration and other analyses have demonstrated that **24** can selectively detect Pb^{2+} with a low LOD (2.7 nM) in acetonitrile media at a binding ratio of 1:1. The pH studies in HEPES media have revealed its very weak fluorescent emission in the pH range of 6.0–13.0 and strong fluorescence in acidic conditions (pH < 6.0). Moreover, recovery tests on real sea shells (clams, pectinids, conches, and oysters) have shown a good recovery ranging from 91.3% to 93.5% [64].



Scheme 24. Chemosensor **24** 2,2''-(((1*E*,1'*E*)-(2-hydroxy-5-methyl-1,3-phenylene)bis(methaneylylidene))bis(azaneylylidene))bis(ethane-2,1-diyl))bis(3',6'-bis(ethylamino)-2',7'-dimethylspiro[isindoline-1,9'-xanthen]-3-one) and its complex with the target metal ion.

Rhodamine B-based compounds conjugated with a polyhydroxy group are generally good detectors for Cu^{2+} , which supports the importance of polyhydroxy substituents as a detecting material for this metal ion. The condensation reaction between Rhodamine B hydrazide and 2,4,6-trihydroxybenzaldehyde yields the sensing material **25** (Scheme 25). Sensing material **25** has a spirolactam structure, as proven by the perpendicular orientation of its xanthen and lactam moiety. Upon addition of various heavy metal ions, only Cu^{2+} has shown an observable color change from colorless to pink with appearance of new absorption band centered at 559 nm. This occurs because the closed spirolactam ring of **25** is opened when adding Cu^{2+} at a 1:1 binding stoichiometry. Sensing material **25** does not show a fluorescence response, which is presumably due to the paramagnetic nature of Cu^{2+} . However, chemosensor **25** presents significant performance in the pH range of 4.0–12.0 for Cu^{2+} , suggesting wide applicability in various environments. Its LOD for Cu^{2+} is 0.48 μM , confirming its good sensitivity [65].



Scheme 25. Chemosensor **25** (*E*)-3',6'-bis(diethylamino)-2',7'-dimethyl-2-((2,4,6-trihydroxybenzylidene)amino)spiro[isindoline-1,9'-xanthen]-3-one and its complex with the target metal ion.

Table 1. Basic quality assurance and analytical parameters for the analysis of metal ions.

Sensing Material	Target Ion(s)	Colorimetric	Fluorescent	Limit of Detection	Solvent Medium	Applications	Ref.
1	Hg ²⁺	Yes	No	-	Organic solvent	-	[32]
2	Hg ²⁺	Yes	No	-	H ₂ O/CH ₃ CN (1:1, v/v)	Test in 10 commercially available Hg ₂ ⁺ compounds	[44]
3	Hg ²⁺	Yes	No	-	H ₂ O/CH ₃ CN (1:1, v/v)	-	[33]
4	Hg ²⁺	Yes	No	-	CH ₃ CN/CH ₂ Cl ₂ (1:1, v/v)	-	[34]
5	Hg ²⁺	No	Yes	1 μM	DMSO ¹⁾	Cosmetics	[45]
6	Hg ²⁺	Yes	Yes	28 nM (Hg ²⁺), 7.5 nM (Cu ²⁺)	CH ₃ CN/H ₂ O (1:1, v/v) and HEPES buffer	Molecular logic gate	[46]
7	Cr ³⁺	No	Yes	1.5 μM	THF ²⁾ /deionized water (1:1, v/v)	-	[47]
8	Cu ²⁺	No	Yes	1.8 μM	CH ₃ CN/HEPES (3:2, v/v)	Living cells	[48]
9	Ag ⁺	No	Yes	0.128 μM	CH ₃ OH/ H ₂ O (1:1, v/v, HEPES = 50 mM, pH = 7.4)	Living cells, real water	[49]
10	Fe ³⁺	Yes	Yes	16 nM	CH ₃ CN	Molecular logic gate	[50]
11	Fe ³⁺	Yes	No	0.36 μM (Fe ³⁺), 0.37 μM (Fe ²⁺)	DMSO/bis-tris buffer (pH = 7.0)	-	[51]
12	Cu ²⁺ , Co ²⁺	Yes	No	0.19 nM (Cu ²⁺), 0.18 nM (Co ²⁺)	DMSO/bis-tris buffer (9:1, v/v, pH = 7.0)	Test in drinking water and tap water	[52]
13	Cu ²⁺	Yes	No	0.37 μM	DMF ³⁾ / bis-tris buffer (1:5, v/v, 10 mM, pH = 7.0)	Test in 19 different amino acids and peptides	[53]
14	Zn ²⁺	Yes (Fe ²⁺ , Fe ³⁺)	Yes (Zn ²⁺ , Al ³⁺)	1.59 μM (Zn ²⁺), 1.34 μM (Al ³⁺), 0.21 μM (Fe ²⁺), 0.22 μM (Fe ³⁺)	MeOH/bis-tris buffer (9:1, v/v, 10 mM, pH = 7.0, for colorimetric), DMF/bis-tris buffer (9.5:0.5, v/v, 10 mM, pH = 7.0, for fluorescent)	Test in tap water and deionized water	[54]
15	Cu ²⁺	Yes	No	23.5 μM	Acetonitrile/ bis-tris buffer (7:3, v/v, 10 mM, pH = 7.0)	-	[55]
16	Hg ²⁺	No	Yes	0.59 μM	DMSO/bis-tris buffer (8:2, v/v)	Test in 20 different amino acids and peptides	[56]
17	Cu ²⁺	Yes	No	0.90 μM	DMSO/bis-tris buffer (0.01:9.99, v/v)	Detection by simple test kit in aqueous solution	[57]

Table 1. Cont.

Sensing Material	Target Ion(s)	Colorimetric	Fluorescent	Limit of Detection	Solvent Medium	Applications	Ref.
18	Co ²⁺	Yes	No	1.28 μM	Bis-tris buffer/MeOH (9.99:0.01, v/v)	Detection by test kit in bis-tris buffer solution	[58]
19	Al ³⁺	No	Yes	0.193 μM	Bis-tris buffer/MeOH (9.99:0.01, v/v)	Cell imaging test in human dermal fibroblast cells	[59]
20	Fe ³⁺	Yes	Yes	-	CH ₃ CN/ H ₂ O (0.5:9.5, v/v)	Cell imaging in HepG2 cells	[60]
21	Al ³⁺ Fe ³⁺	Yes	Yes	1.18 nM (Al ³⁺), 1.80 nM (Cr ³⁺), 4.04 nM (Fe ³⁺)	10 mM HEPES buffer in methanol:water (7:3, v/v, at pH = 7.2)	Molecular logic devices	[61]
22	Al ³⁺	Yes	Yes	10.98 nM (Al ³⁺), 76.92 nM (Zn ²⁺)	10 mM HEPES buffer in methanol:water (9:1, v/v, at pH = 7.4)	Cell imaging in BV2 cells	[62]
23	Cu ²⁺ , Fe ³⁺	Yes	Yes	18 nM (Cu ²⁺), 33 nM (Fe ³⁺)	Aqueous medium	Biosensing and bioimaging in zebrafish embryos	[63]
24	Pb ²⁺	Yes	Yes	2.7 nM	0.01 M HEPES buffer in water (pH = 7.4)	Detection in sea shell food	[64]
25	Cu ²⁺	Yes	No	480 nM	30% acetonitrile solution	Not suitable as cytotoxic agent for colorectal cancer cells	[65]

¹⁾ DMSO: dimethyl sulfoxide, ²⁾ THF: tetrahydrofuran, ³⁾ DMF: dimethylformamide.

6. Conclusions

High-performance chemosensors can be obtained by fine-tuning the functional groups governing their electron transfer mechanisms such as MLCT, ICT, PET, etc. Since the electron distribution over the receptor and functional group(s) causes fluorescence emission (fluorescent chemosensor) and/or color change (colorimetric chemosensor) upon interaction with metal ions. Therefore, the appropriate functional group should be selected for the desired assay outputs. As extensively discussed in this review, sensing characteristics such as sensitivity, selectivity, LOD, and detection response are significantly affected by the types of functional groups. Pt(dithiolene)-based chemosensors are great examples to explain that the sensing capability can be modified by substituting the electron-donating structures on same receptor. By substituting the electron-donating moiety, the binding affinity with the desired metal ion can be improved, or multiple analytes can be selectively detected in the presence with the coexistence of interfering metal ions in the solution. Schiff base chemosensors exhibit excellent performances due to their unique electron configuration and ease of functional group substitution. Most of Schiff base chemosensors take the advantages of high selectivity and LOD lower than practical regulations; thus, they offer wide applicability in biological and environmental fields. These representative chemosensors are summarized in Table 1. Despite of the recent meaningful development of various chemosensors, an advanced chemosensor with high sensitivity, selectivity, intensity, and sensing response, wide pH range, and applicability to aqueous is still demanded. We hope this review helps researchers to understand the recent state-of-the-art advancements in this field and synthesize their chemosensors by selecting proper functional groups with desired optical properties and suitability for practical applications.

Author Contributions: Conceptualization, D.-Y.N. and I.N.; methodology, J.-K.P., M.-L.S. and J.K.; software, J.S. and S.C.; validation, S.J., H.E., O.K. and S.P.; writing—original draft preparation, J.-K.P., J.S. and S.J.; writing—review and editing, M.-L.S., S.P., D.-Y.N. and I.N.; visualization, J.-K.P., J.S. and S.J.; supervision, D.-Y.N. and I.N.; project administration, D.-Y.N. and I.N. All authors have read and agreed to the published version of the manuscript.

Funding: This paper was supported by the Commercialization Promotion Agency for R&D Outcomes (COMP A) funded by the Korea Government (MSIT) (2021-RMD-S05), the Korea Institute of Energy Technology Evaluation and Planning (KETEP) funded by the Korea Government (MOTIE) (No. 20214000000280), the Chung-Ang University Graduate Research Scholarship in 2022, and a research grant from Seoul Women's University (2022-0442).

Conflicts of Interest: The authors declare no conflict of interest.

References

1. Fang, Y.; Dehaen, W. Small-molecule-based fluorescent probes for f-block metal ions: A new frontier in chemosensors. *Coord. Chem. Rev.* **2021**, *427*, 213524. [[CrossRef](#)]
2. Boening, D.W. Ecological effects, transport, and fate of mercury: A general review. *Chemosphere* **2000**, *40*, 1335–1351. [[CrossRef](#)]
3. Bolger, P.M.; Schwetz, B. Mercury and health. *N. Engl. J. Med.* **2002**, *347*, 1735–1736. [[CrossRef](#)]
4. Clarkson, T.W. The Toxicology of Mercury. *Crit. Rev. Clin. Lab. Sci.* **1997**, *34*, 369–403. [[CrossRef](#)] [[PubMed](#)]
5. Naik, L.; Maridevarmath, C.V.; Thippeswamy, M.S.; Savanur, H.M.; Khazi, I.A.M.; Malimath, G.H. A highly selective and sensitive thiophene substituted 1,3,4-oxadiazole based turn-off fluorescence chemosensor for Fe²⁺ and turn on fluorescence chemosensor for Ni²⁺ and Cu²⁺ detection. *Mater. Chem. Phys.* **2021**, *260*, 124063. [[CrossRef](#)]
6. Wang, L.; Gong, X.; Bing, Q.; Wang, G. A new oxadiazole-based dual-mode chemosensor: Colorimetric detection of Co²⁺ and fluorometric detection of Cu²⁺ with high selectivity and sensitivity. *Microchem. J.* **2018**, *142*, 279–287. [[CrossRef](#)]
7. Saeed, T.S.; Maddipatla, D.; Narakathu, B.B.; Albalawi, S.S.; Obare, S.O.; Atashbar, M.Z. Synthesis of a novel hexaazatriphenylene derivative for the selective detection of copper ions in aqueous solution. *RSC Adv.* **2019**, *9*, 39824–39833. [[CrossRef](#)] [[PubMed](#)]
8. Ozdemir, M. A novel chromogenic molecular sensing platform for highly sensitive and selective detection of Cu²⁺ ions in aqueous environment. *J. Photochem. Photobiol. A: Chem.* **2019**, *369*, 54–69. [[CrossRef](#)]
9. Harikrishnan, M.; Sadhasivam, V.; Mariyappan, M.; Murugesan, S.; Malini, N.; Siva, A. A simple triazine (D-A) based organic fluorophore selective dual sensor for Copper(II) and dichromate ions and its solvatochromism, solid state sensing, logic gate applications. *Dye. Pigment.* **2019**, *168*, 123–133. [[CrossRef](#)]
10. Barnham, K.J.; Bush, A.I. Metals in Alzheimer's and Parkinson's Diseases. *Curr. Opin. Chem. Biol.* **2008**, *12*, 222–228. [[CrossRef](#)]
11. Gaggelli, E.; Kozłowski, H.; Valensin, D.; Valensin, G. Copper Homeostasis and Neurodegenerative Disorders (Alzheimer's, Prion, and Parkinson's Diseases and Amyotrophic Lateral Sclerosis). *Chem. Rev.* **2006**, *106*, 1995–2044. [[CrossRef](#)] [[PubMed](#)]
12. Kozłowski, H.; Luczkowski, M.; Remelli, M.; Valensin, D. Copper, zinc and iron in neurodegenerative diseases (Alzheimer's, Parkinson's and prion diseases). *Coord. Chem. Rev.* **2012**, *256*, 2129–2141. [[CrossRef](#)]
13. Zhu, M.; Yuan, M.; Liu, X.; Xu, J.; Lv, J.; Huang, C.; Liu, H.; Li, Y.; Wang, S.; Zhu, D. Visible near-infrared chemosensor for mercury ion. *Org. Lett.* **2008**, *10*, 1481–1484. [[CrossRef](#)] [[PubMed](#)]
14. Dongare, P.R.; Gore, A.H. Recent Advances in Colorimetric and Fluorescent Chemosensors for Ionic Species: Design, Principle and Optical Signalling Mechanism. *Chem. Sel.* **2021**, *6*, 5657–5669. [[CrossRef](#)]
15. Valeur, B.; Leray, I. Design principles of fluorescent molecular sensors for cation recognition. *Coord. Chem. Rev.* **2000**, *205*, 3–40. [[CrossRef](#)]
16. Wu, J.; Liu, W.; Ge, J.; Zhang, H.; Wang, P. New sensing mechanisms for design of fluorescent chemosensors emerging in recent years. *Chem. Soc. Rev.* **2011**, *40*, 3483–3495. [[CrossRef](#)]
17. Kaur, B.; Kaur, N.; Kumar, S. Colorimetric metal ion sensors—A comprehensive review of the years 2011–2016. *Coord. Chem. Rev.* **2018**, *358*, 13–69. [[CrossRef](#)]
18. Valeur, B.; Berberan-Santos, M.N. *Molecular Fluorescence: Principles and Applications*; John Wiley & Sons: Hoboken, NJ, USA, 2012.
19. Roy, P. Recent advances in the development of fluorescent chemosensors for Al³⁺. *Dalton Trans.* **2021**, *50*, 7156–7165. [[CrossRef](#)] [[PubMed](#)]
20. Bhalla, P.; Malhotra, K.; Tomer, N.; Malhotra, R. Binding interactions and Sensing applications of chromone derived Schiff base chemosensors via absorption and emission studies: A comprehensive review. *Inorg. Chem. Commun.* **2022**, *146*, 110026. [[CrossRef](#)]
21. de Silva, A.P.; Gunaratne, H.Q.N.; Gunnlaugsson, T.; Huxley, A.J.M.; McCoy, C.P.; Rademacher, J.T.; Rice, T.E. Signaling Recognition Events with Fluorescent Sensors and Switches. *Chem. Rev.* **1997**, *97*, 1515–1566. [[CrossRef](#)]
22. Callan, J.F.; de Silva, A.P.; Magri, D.C. Luminescent sensors and switches in the early 21st century. *Tetrahedron* **2005**, *61*, 8551–8588. [[CrossRef](#)]
23. Martínez-Mañez, R.; Sancenón, F. Fluorogenic and Chromogenic Chemosensors and Reagents for Anions. *Chem. Rev.* **2003**, *103*, 4419–4476. [[CrossRef](#)] [[PubMed](#)]
24. Xu, Z.; Yoon, J.; Spring, D.R. Fluorescent chemosensors for Zn²⁺. *Chem. Soc. Rev.* **2010**, *39*, 1996–2006. [[CrossRef](#)]
25. Kim, J.S.; Quang, D.T. Calixarene-Derived Fluorescent Probes. *Chem. Rev.* **2007**, *107*, 3780–3799. [[CrossRef](#)] [[PubMed](#)]
26. Gunnlaugsson, T.; Ali, H.D.P.; Glynn, M.; Kruger, P.E.; Hussey, G.M.; Pfeffer, F.M.; dos Santos, C.M.G.; Tierney, J. Fluorescent Photoinduced Electron Transfer (PET) Sensors for Anions; From Design to Potential Application. *J. Fluoresc.* **2005**, *15*, 287–299. [[CrossRef](#)] [[PubMed](#)]
27. Zhao, Q.; Li, F.; Huang, C. Phosphorescent chemosensors based on heavy-metal complexes. *Chem. Soc. Rev.* **2010**, *39*, 3007–3030. [[CrossRef](#)]

28. Wu, J.-S.; Liu, W.-M.; Zhuang, X.-Q.; Wang, F.; Wang, P.-F.; Tao, S.-L.; Zhang, X.-H.; Wu, S.-K.; Lee, S.-T. Fluorescence Turn On of Coumarin Derivatives by Metal Cations: A New Signaling Mechanism Based on C=N Isomerization. *Org. Lett.* **2007**, *9*, 33–36. [[CrossRef](#)]
29. Li, J.-Y.; Zhou, X.-Q.; Zhou, Y.; Fang, Y.; Yao, C. A highly specific tetrazole-based chemosensor for fluoride ion: A new sensing functional group based on intramolecular proton transfer. *Spectrochim. Acta Part A Mol. Biomol. Spectrosc.* **2013**, *102*, 66–70. [[CrossRef](#)] [[PubMed](#)]
30. Sasaki, S.-I.; Kotegawa, Y.; Tamiaki, H. Trifluoroacetyl-chlorin as a new chemosensor for alcohol/amine detection. *Tetrahedron Lett.* **2006**, *47*, 4849–4852. [[CrossRef](#)]
31. Jiang, W.; Fu, Q.; Fan, H.; Ho, J.; Wang, W. A Highly Selective Fluorescent Probe for Thiophenols. *Angew. Chem. Int. Ed.* **2007**, *46*, 8445–8448. [[CrossRef](#)] [[PubMed](#)]
32. Jeon, H.; Suh, W.; Noh, D.-Y. Hg (II) sensing properties of (diphosphine) Pt (dmit) complexes (dmit: C3S52–: 1, 3-dithiole-2-thione-4, 5-dithiolate). *Inorg. Chem. Commun.* **2012**, *24*, 181–185. [[CrossRef](#)]
33. Jeon, H.; Ryu, H.; Nam, I.; Noh, D.-Y. Heteroleptic Pt(II)-dithiolene-based Colorimetric Chemosensors: Selectivity Control for Hg(II) Ion Sensing. *Materials* **2020**, *13*, 1385. [[CrossRef](#)] [[PubMed](#)]
34. Son, H.; Jang, S.; Lim, G.; Kim, T.; Nam, I.; Noh, D.-Y. Pt(dithiolene)-Based Colorimetric Chemosensors for Multiple Metal-Ion Sensing. *Sustainability* **2021**, *13*, 8160. [[CrossRef](#)]
35. Abu-Dief, A.M.; Mohamed, I.M.A. A review on versatile applications of transition metal complexes incorporating Schiff bases. *Beni-Suef Univ. J. Basic Appl. Sci.* **2015**, *4*, 119–133. [[CrossRef](#)] [[PubMed](#)]
36. Berhanu, A.L.; Gaurav; Mohiuddin, I.; Malik, A.K.; Aulakh, J.S.; Kumar, V.; Kim, K.-H. A review of the applications of Schiff bases as optical chemical sensors. *TrAC Trends Anal. Chem.* **2019**, *116*, 74–91. [[CrossRef](#)]
37. Goshisht, M.K.; Patra, G.K.; Tripathi, N. Fluorescent Schiff base sensors as a versatile tool for metal ion detection: Strategies, mechanistic insights, and applications. *Mater. Adv.* **2022**, *3*, 2612–2669. [[CrossRef](#)]
38. Kumar, M.; Kumar, A.; Kishor, S.; Kumar, S.; Kumar, A.; Manav, N.; Bhagi, A.K.; Kumar, S.; John, R.P. N-diethylaminosalicylidene based “turn-on” fluorescent Schiff base chemosensor for Al³⁺ ion: Synthesis, characterisation and DFT/TD-DFT studies. *J. Mol. Struct.* **2022**, *1247*, 131257. [[CrossRef](#)]
39. Khan, S.; Chen, X.; Almahri, A.; Allehyani, E.S.; Alhumaydhi, F.A.; Ibrahim, M.M.; Ali, S. Recent developments in fluorescent and colorimetric chemosensors based on schiff bases for metallic cations detection: A review. *J. Environ. Chem. Eng.* **2021**, *9*, 106381. [[CrossRef](#)]
40. Tidwell, T.T. Hugo (Ugo) Schiff, Schiff Bases, and a Century of β -Lactam Synthesis. *Angew. Chem. Int. Ed.* **2008**, *47*, 1016–1020. [[CrossRef](#)]
41. Zafar, H.; Ahmad, A.; Khan, A.U.; Khan, T.A. Synthesis, characterization and antimicrobial studies of Schiff base complexes. *J. Mol. Struct.* **2015**, *1097*, 129–135. [[CrossRef](#)]
42. Gupta, V.K.; Singh, A.K.; Kumawat, L.K. Thiazole Schiff base turn-on fluorescent chemosensor for Al³⁺ ion. *Sens. Actuators B: Chem.* **2014**, *195*, 98–108. [[CrossRef](#)]
43. Sun, J.; Ye, B.; Xia, G.; Wang, H. A multi-responsive squaraine-based “turn on” fluorescent chemosensor for highly sensitive detection of Al³⁺, Zn²⁺ and Cd²⁺ in aqueous media and its biological application. *Sens. Actuators B: Chem.* **2017**, *249*, 386–394. [[CrossRef](#)]
44. Jeon, S.; Suh, W.; Noh, D.-Y. Anion-dependent Hg²⁺-sensing of colorimetric (dppe)Pt(dmit) chemosensor (dppe: 1,2-bis(diphenylphosphino)ethane; dmit: 1,3-dithiole-2-thione-4,5-dithiolate). *Inorg. Chem. Commun.* **2017**, *81*, 43–46. [[CrossRef](#)]
45. Sun, T.; Niu, Q.; Li, Y.; Li, T.; Liu, H. Novel oligothiophene-based dual-mode chemosensor: “Naked-Eye” colorimetric recognition of Hg²⁺ and sequential off-on fluorescence detection of Fe³⁺ and Hg²⁺ in aqueous media and its application in practical samples. *Sens. Actuators B: Chem.* **2017**, *248*, 24–34. [[CrossRef](#)]
46. Razi, S.S.; Ali, R.; Gupta, R.C.; Dwivedi, S.K.; Sharma, G.; Koch, B.; Misra, A. Phenyl-end-capped-thiophene (P-T type) based ICT fluorescent probe (D– π –A) for detection of Hg²⁺ and Cu²⁺ ions: Live cell imaging and logic operation at molecular level. *J. Photochem. Photobiol. A: Chem.* **2016**, *324*, 106–116. [[CrossRef](#)]
47. Kolcu, F.; Erdener, D.; Kaya, İ. A Schiff base based on triphenylamine and thiophene moieties as a fluorescent sensor for Cr (III) ions: Synthesis, characterization and fluorescent applications. *Inorg. Chim. Acta* **2020**, *509*, 119676. [[CrossRef](#)]
48. He, G.; Liu, C.; Liu, X.; Wang, Q.; Fan, A.; Wang, S.; Qian, X. Design and synthesis of a fluorescent probe based on naphthalene anhydride and its detection of copper ions. *PLoS ONE* **2017**, *12*, e0186994. [[CrossRef](#)] [[PubMed](#)]
49. Bhuvanesh, N.; Suresh, S.; Kumar, P.R.; Mothi, E.M.; Kannan, K.; Kannan, V.R.; Nandhakumar, R. Small molecule “turn on” fluorescent probe for silver ion and application to bioimaging. *J. Photochem. Photobiol. A: Chem.* **2018**, *360*, 6–12. [[CrossRef](#)]
50. Harsha, K.G.; Ananda Rao, B.; Baggi, T.R.; Prabhakar, S.; Jayathirtha Rao, V. Thiophene-phenylquinazoline probe for selective ratiometric fluorescence and visual detection of Fe(III) and turn-off fluorescence for I[–] and its applications. *Photochem. Photobiol. Sci.* **2020**, *19*, 1707–1716. [[CrossRef](#)]
51. Chae, J.B.; Jang, H.J.; Kim, C. Sequential detection of Fe^{3+/2+} and pyrophosphate by a colorimetric chemosensor in a near-perfect aqueous solution. *Photochem. Photobiol. Sci.* **2017**, *16*, 1812–1820. [[CrossRef](#)]
52. Min, C.H.; Na, S.; Shin, J.E.; Kim, J.K.; Jo, T.G.; Kim, C. A new Schiff-based chemosensor for chromogenic sensing of Cu²⁺, Co²⁺ and S^{2–} in aqueous solution: Experimental and theoretical studies. *New J. Chem.* **2017**, *41*, 3991–3999. [[CrossRef](#)]

53. Kim, Y.S.; Park, G.J.; Lee, S.A.; Kim, C. A colorimetric chemosensor for the sequential detection of copper ion and amino acids (cysteine and histidine) in aqueous solution. *RSC Adv.* **2015**, *5*, 31179–31188. [[CrossRef](#)]
54. Kim, Y.S.; Park, G.J.; Lee, J.J.; Lee, S.Y.; Lee, S.Y.; Kim, C. Multiple target chemosensor: A fluorescent sensor for Zn(ii) and Al(iii) and a chromogenic sensor for Fe(ii) and Fe(iii). *RSC Adv.* **2015**, *5*, 11229–11239. [[CrossRef](#)]
55. Choi, Y.W.; Lee, J.J.; You, G.R.; Lee, S.Y.; Kim, C. Chromogenic naked-eye detection of copper ion and fluoride. *RSC Adv.* **2015**, *5*, 86463–86472. [[CrossRef](#)]
56. You, G.R.; Lee, S.Y.; Lee, J.J.; Kim, Y.S.; Kim, C. Sequential detection of mercury(ii) and thiol-containing amino acids by a fluorescent chemosensor. *RSC Adv.* **2016**, *6*, 4212–4220. [[CrossRef](#)]
57. You, G.R.; Park, G.J.; Lee, J.J.; Kim, C. A colorimetric sensor for the sequential detection of Cu²⁺ and CN[−] in fully aqueous media: Practical performance of Cu²⁺. *Dalton Trans.* **2015**, *44*, 9120–9129. [[CrossRef](#)]
58. Park, G.J.; Na, Y.J.; Jo, H.Y.; Lee, S.A.; Kim, C. A colorimetric organic chemo-sensor for Co²⁺ in a fully aqueous environment. *Dalton Trans.* **2014**, *43*, 6618–6622. [[CrossRef](#)]
59. Lee, S.A.; You, G.R.; Choi, Y.W.; Jo, H.Y.; Kim, A.R.; Noh, I.; Kim, S.-J.; Kim, Y.; Kim, C. A new multifunctional Schiff base as a fluorescence sensor for Al³⁺ and a colorimetric sensor for CN[−] in aqueous media: An application to bioimaging. *Dalton Trans.* **2014**, *43*, 6650–6659. [[CrossRef](#)]
60. Lee, M.H.; Lee, H.; Chang, M.J.; Kim, H.S.; Kang, C.; Kim, J.S. A fluorescent probe for the Fe³⁺ ion pool in endoplasmic reticulum in liver cells. *Dye Pigments* **2016**, *130*, 245–250. [[CrossRef](#)]
61. Dey, S.; Sarkar, S.; Maity, D.; Roy, P. Rhodamine based chemosensor for trivalent cations: Synthesis, spectral properties, secondary complex as sensor for arsenate and molecular logic gates. *Sens. Actuators B: Chem.* **2017**, *246*, 518–534. [[CrossRef](#)]
62. Roy, A.; Shee, U.; Mukherjee, A.; Mandal, S.K.; Roy, P. Rhodamine-Based Dual Chemosensor for Al³⁺ and Zn²⁺ Ions with Distinctly Separated Excitation and Emission Wavelengths. *ACS Omega* **2019**, *4*, 6864–6875. [[CrossRef](#)]
63. Senthil Murugan, A.; Vidhyalakshmi, N.; Ramesh, U.; Annaraj, J. In vivo bio-imaging studies of highly selective, sensitive rhodamine based fluorescent chemosensor for the detection of Cu²⁺/Fe³⁺ ions. *Sens. Actuators B: Chem.* **2018**, *274*, 22–29. [[CrossRef](#)]
64. Wan, J.; Zhang, K.; Li, C.; Li, Y.; Niu, S. A novel fluorescent chemosensor based on a rhodamine 6G derivative for the detection of Pb²⁺ ion. *Sens. Actuators B: Chem.* **2017**, *246*, 696–702. [[CrossRef](#)]
65. Cheah, P.W.; Heng, M.P.; Saad, H.M.; Sim, K.S.; Tan, K.W. Specific detection of Cu²⁺ by a pH-independent colorimetric rhodamine based chemosensor. *Opt. Mater.* **2021**, *114*, 110990. [[CrossRef](#)]